Proceedings of the 2nd Marine Energy Technology Symposium
METS2014
April 15-18, 2014, Seattle, WA

SIMULATION OF HYDROKINETIC TURBINES IN TURBULENT FLOW USING VORTEX PARTICLE METHODS

Danny Sale[1], Alberto Aliseda[2]
University of Washington
Dept. of Mechanical Engineering
Seattle, WA, U.S.A.
[1] dsale@uw.edu [2] aaliseda@uw.edu

Ye Li
Shanghai Jiao Tong University
School of Naval Architecture, Ocean and Civil Engineering
Shanghai 200240, China

ABSTRACT

This work presents the development of computational models that capture vorticity generation and turbulent diffusion within wind and hydrokinetic turbine farms. The use of vortex methods is examined as an alternative for modeling turbulent wakes and rotor-wake interaction. The vorticity-velocity formulation of the Navier-Stokes equations are simulated by a hybrid Lagrangian-Eulerian method involving both fluid particles that carry vorticity and mesh discretizations which enable an efficient solution to N-body vorticity dynamics. A "mesh free" particle-strength-exchange (PSE) algorithm and a "particle-mesh" vortex-in-cell (VIC) algorithm are implemented for a series of benchmarks to verify the simulation method for low Reynolds number flows, including: vortex ring dynamics, flow over bluff bodies, and a 3D wing. These examples are presented on a variety of computer architectures, with support for distributed-memory parallelism, multi-core, and GPGPU computing. The scalability and stability of these proposed vortex methods shows potential for modeling the large range of scales present between rotor-scale and farm-scale hydrodynamics. The desired feature of this methodology is faithful prediction of unsteady phenomenon, capture of vortex shedding, and tracking the evolution of vortical structures as they evolve and interact with immersed structures and ambient turbulent flow.

1. INTRODUCTION

Marine renewable energy is advancing towards commercialization, including electrical power generation from ocean waves, wind and tidal currents. Figure 1 illustrates hydrokinetic turbine models that are currently undergoing laboratory scale testing activities in the United States directed by the US Department of Energy [1]. The effective and safe design of **M**arine **E**nergy **C**onverters (MECs) to harness the energy in flowing water requires detailed knowledge of the mean velocity, turbulence, and wave characteristics. Operating in turbulent conditions can contribute to higher maintenance costs and is associated with lower energy production, and accurate representation of the turbulent spectrum is critical to understand the transfer of energy from the turbulence to the MEC and support structure.

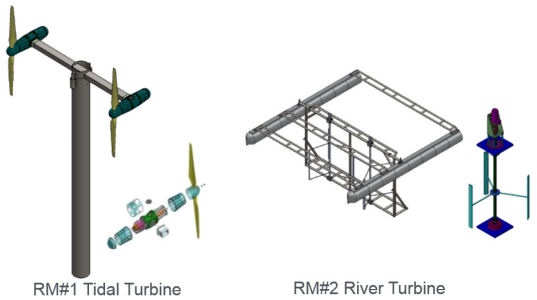

FIGURE 1. REFERENCE MODELS FOR TIDAL AND RIVER HYDROKINETIC TURBINES [1].

In the present work, the focus is twofold: (1) A three-dimensional vortex method development to serve as a hydrodynamic analysis tool for single MEC devices. This hydrodynamic analysis will capture the unsteady forces caused by atmospheric turbulence and rotor-wake interactions, recover pressure distributions for coupled structural analysis, and be generalizable to complex geometries (e.g. rotor blades with built-in curvature, bluff bodies). (2) Development of a scalable computational framework for this vortex method to take advantage of shared- and distributed-memory parallel computer architectures, including general-purpose computing on graphics processing units (GPGPU). The capability to model farm-scale hydrodynamics with multiple MECs is envisioned.

1.1) Review of Current Approaches

First, a summary is given on the most successful methods in computational fluids applied in the design of wind and hydrokinetic turbines [2,3]. The wind turbine certification process (and presumably the hydrokinetic turbine process will too) can require simulation of 1000's of different operational scenarios that a turbine may

experience over its lifetime. The blade element momentum theory (BEMT) and Generalized Dynamic Wake (GDW) methods remain the most widely used methods in the engineering of renewable energy turbines, thanks to their computational speed and acceptable accuracy. However, detailed analysis of the surrounding flow field requires solution of the Euler or Navier-Stokes equations, which lead to the development of panel/vortex (integral boundary element) methods and application of Reynolds-Averaged Navier-Stokes (RANS) / Large Eddy Simulation (LES) methods.

The blade element momentum theory (BEMT) is a simple 2D steady flow method that is commonly used early in the design process of wind and marine hydrokinetic (MHK) turbines. There are numerous empirical corrections that can be used to account for three dimensional and unsteady flow phenomena such as tip/hub losses, skewed/rotating wake, stall-delay, and dynamic stall hysteresis. Variants of the BEMT have also been developed for vertical axis turbines using the double streamtube formulation that takes the front and the back halves of the turbine swept cylinder as separate elements that takes momentum and kinetic energy from the flow. Unsteady formulations of the BEMT have also been developed to account for the influence of spatially varying flow over the rotor disk.

Generalized Dynamic Wake (GDW) theory, also known as the "acceleration potential method" was originally developed for the helicopter industry to evaluate performance and dynamics in a simplified flight control setting. GDW is based on a potential flow solution to Laplace's equation which is used to develop the equations for the pressure distributions in the rotor plane. An advantage over BEMT is that GDW allows for a more general distribution of pressure across a rotor plane than BEMT. Other key advantages of the GDW method over BEMT include inherent modeling of the dynamic wake effect, tip losses, and skewed wake aerodynamics [2, 3]. The dynamic wake effect refers to influence on wake development imposed by the time lag in the induced velocities created by the vorticity being shed from the blades before being convected downstream. There are limitations shared by BEMT and GDW based on the simplifications it assumes in the flow field around turbine rotors: both assume the rotor disk is flat and therefore wake aerodynamics will not be accurately modeled when there exist large aeroelastic deflections, significant coning and/or pre-curvature built into the blades. Furthermore, the GDW does not include rotation in the wake, and becomes unstable at lower flow speeds, due to the assumption of lightly loaded rotors.

Panel methods are widely used in the aeronautics industry for predesign of lifting surfaces on aircraft. They model the turbine blades as a lifting surface that sheds a vortex sheet constructed from a lattice of vortex filaments to form the wake. A shortcoming of this approach is that numerical error accumulates in regions where vortex filaments develop high curvature, as the wake mixes and diffuses into the ambient flow. The vortex lattice wake, which depends on the Euler equations, cannot represent a fully turbulent flow due to inviscid assumptions. Accumulation of numerical error as the wake mesh becomes entangled (Lagrangian distortion) quickly increases the cost and reduces the accuracy of the method.

Single reference method, sliding mesh methods, in combination with RANS or LES flow field solvers, can use the full rotor geometry representation to investigate the details of the flow field and the influence of complex topography/incoming flow field on MHK turbine performance. These methods are becoming common practice as computational power increases. RANS solvers rely on turbulence modeling over the entire turbulence spectrum due to closure problem of the averaged equations, and closure models can have difficulties predicting separated flow. LES is able to resolve partially into the inertial range of the turbulent spectrum, while the remaining smaller and more isotropic turbulence must be predicted with a subfilter-scale turbulence model. LES is able to more accurately resolve separated flows and incorporate more physics than RANS, but subfilter-scale models still have significant challenges in the presence of solid walls, stratification, rotation, and large shear layers that are not resolved by the LES grid. The computational cost of RANS and LES can be reduced with the use of actuator disks/lines/surface methods to implement the turbine rotor as body forces in the momentum equations, without having a physical representation of the blade geometry on the computational mesh. These simplified methods for turbine representation can then be used to simulate arrays of turbines and wind farm dynamics, even including oceanic and atmospheric turbulence [5, 6, 24]. The accuracy of any aforementioned blade-element method relies on lookup tables of aerodynamic coefficients and is most sensitive to the quality and careful preparation of the airfoil data.

1.2) Motivation for Vortex Particle Method

The focus of this computational effort is to understand the fluid-structure interaction of flow around an MHK turbine in a large domain, and under the influence of other turbine wakes. This requires an accurate representation of unsteady and separated flows in a fast and stable method that can handle long simulation times. Vortex methods have a large variety of formulations, ranging from simpler engineering models [17] to LES and DNS counterparts [6].

Accurate representation of the turbulent spectrum is critical to understand the transfer of energy from the turbulence to the rotor and support structure and its strong effect on turbine performance and fatigue [4]. Often this means that it is necessary to resolve the flow field at length scales smaller than the chord length of the blades, requiring increased computational cost. Eulerian formulations in CFD rely on construction of a computational mesh that can be difficult and time consuming, especially when moving objects with complex geometries are immersed in the fluid. Furthermore, these formulations, particularly LES, encounter difficulties when applied to high Reynolds number flows (upwards of 10^6) because of the requirement for fine resolution grids in order to obtain resolution of the turbulence structures. In particle methods the number of computational elements also needs to be increased when higher resolution of turbulence structures is required, but the vorticity field for external flows and wakes is compact and computational elements are required only in regions of the domain occupied by vorticity. This can enable vortex methods to represent the same flow using fewer computational elements and without blockage effects due to presence of numerical boundaries. Furthermore, the Lagrangian nature of vortex methods are less limited by the Courant–Friedrichs–Lewy condition (CFL number), and can enjoy taking larger time steps compared to purely Eulerian formulations.

As an alternative to turbulence modeling used in RANS and LES, vortex methods can account for underresolved subgrid scales by so-called vorticity redistribution schemes. Vorticity redistribution schemes enable vortex methods to behave as LES models, in the sense that they avoid accumulation of energy at the high wavenumber end of the spectrum, and avoid excessive dissipation in the resolved scales [7,8,9]. Vorticity redistribution amounts to interpolation of the particle strengths onto an underlying Eulerian mesh that allows highly distorted particles to be split into multiple particles, or creation of particles at smaller scales when needed. Lastly, numerical schemes and turbulence models have been less developed for vorticity formulations, and this may explain that recent simulation of turbine wakes are performed using the primitive variable approaches (velocity-pressure formulations). Particle methods offer natural and intuitive ways to deal with multiple scales in a problem, and have been successfully applied in fields of fluid and solid mechanics [18]. Construction of adaptive schemes for particle methods has received much attention in recent years, and particle methods are well suited to exploit new hardware technologies that are revolutionizing the high-performance computing scene [10,11].

2. VORTEX PARTICLE METHODS

The class of three-dimensional vortex particle methods described in [8,9] and references within is followed in this work. In flows dominated by vorticity, it can be advantageous to work in the velocity-vorticity formulation of the Navier-Stokes (N-S) equations

$$\frac{D\boldsymbol{\omega}}{Dt} = \frac{\partial \boldsymbol{\omega}}{\partial \mathrm{t}} + \boldsymbol{u}\cdot\boldsymbol{\nabla\omega} = \boldsymbol{\omega}\cdot\boldsymbol{\nabla}\mathbf{u} + \nu\boldsymbol{\nabla}^2\boldsymbol{\omega} \qquad (1)$$

where velocity and vorticity are related by $\boldsymbol{\omega} = \boldsymbol{\nabla}\times\boldsymbol{u}$ and ν is the fluid kinematic viscosity. Since the pressure term is decoupled in this form, the difficulty associated with pressure-velocity coupling is removed. The pressure is not part of the solution algorithm, and can be obtained in a post-processing step via solution of an additional pressure Poisson equation.

The vortex particle method approximates the continuous vorticity field by a set of discrete particles, representing fluid elements carrying Gaussian shaped distributions of vorticity. The width of the vorticity distribution for a single particle is a parameter (usually chosen as a constant) that controls the length scale for which the velocity field is resolved—this parameter provides an approximate classification of the unresolved sub-grid scales. A particle is a modified Dirac's delta distribution centered at position $\mathbf{x}^p$ and carrying a vectorized strength $\boldsymbol{\alpha}^p = vol^p\boldsymbol{\omega}^p$, referred to as circulation. For incompressible flows, the particle volumes vol^p do not evolve in time and an additional equation for tracking particle volumes is not required. Particles usually have equal volume of fluid; for example, initializing particles on a $\boldsymbol{h\,x\,h\,x\,h}$ lattice gives $\boldsymbol{vol} = \boldsymbol{h^3}$ divided equally among particles. Furthermore, the shape of the particle volumes is unimportant due to the assumption that

quantities are constant inside a particle's support. The approximation to the vorticity field is then given by the summation of all particle contributions

$$\boldsymbol{\omega}(\mathbf{x},t)=\sum_{p}\boldsymbol{\alpha}^{p}(t)\zeta_{\sigma}\left(\mathbf{x}-\mathbf{x}^{p}(t)\right) \qquad (2)$$

$$\zeta_{\sigma}(\mathbf{x})=\frac{1}{\sigma^{3}}\zeta(\frac{|\mathbf{x}|}{\sigma}). \qquad (3)$$

where ζ_{σ} is a regularization function chosen usually as radially symmetric, and σ is a parameter defining the characteristic width (or core size) of the vortex particle. There are many choices for the smoothing function $\zeta(\boldsymbol{x})$, usually of Gaussian shape, and which affects the spatial accuracy of the method. Examples of different formulations of ζ_{σ} are tabulated in [7] along with corresponding spatial accuracy and conservation properties.

The fluid elements move with the corresponding local velocity, and thus the fluid simulation amounts to tracking the dynamics of N particles governed by ordinary differential equations, (4) and (5), that determine the trajectories of the particle positions $\mathbf{x}^{p}$ and the evolution of particle circulations $\boldsymbol{\alpha}^{p}$ due to vortex stretching and diffusion. In principle, these ODEs can be solved using classical time stepping schemes such as Runge-Kutta or multistep methods.

$$\frac{d\boldsymbol{x}^{p}}{dt}=\boldsymbol{u}(\mathbf{x}^{p}(t),t) \qquad (4)$$

$$\frac{d\boldsymbol{\alpha}^{p}}{dt}=\boldsymbol{\alpha}^{p}\cdot\nabla\mathbf{u}(\mathbf{x}^{p},\mathrm{t})+\nu\nabla^{2}\boldsymbol{\alpha}^{p} \qquad (5)$$

For many engineering applications, one can argue that the properties of the flow are only changing rapidly in small regions of the flow and are constant in large regions of the flow—this motivates an approach based on Helmholtz decomposition of the flow into rotational (vorticity containing $\boldsymbol{u}_{\boldsymbol{\omega}}$) and irrotational velocity components (potential flow $\boldsymbol{u}_{\Phi}=\boldsymbol{\nabla}\Phi$ and freestream velocity $\boldsymbol{U}_{\infty}$). Inserting the particle approximation (Eqn. 2) into the Biot-Savart law gives the rotational contribution to the velocity field (Eqn. 7). The condition of incompressible flow $(\boldsymbol{\nabla}\cdot\boldsymbol{u}=0)$ ensures the existence of the solenoidal vector potential referred to as the stream function Ψ $\boldsymbol{(\nabla\cdot\Psi=0)}$ related to the velocity and vorticity through Equations 8 and 9. Equations 9 and 10 are the Poisson equations for the stream function and rotational velocity field.

$$\boldsymbol{u}=\boldsymbol{u}_{\boldsymbol{\omega}}+\boldsymbol{u}_{\Phi}+\boldsymbol{U}_{\infty} \qquad (6)$$

$$\boldsymbol{u}_{\boldsymbol{\omega}}(\mathbf{x},t)=-\frac{1}{4\pi}\sum_{p}\frac{\mathbf{x}-\mathbf{x}^{\boldsymbol{p}}(\boldsymbol{t})}{|\mathbf{x}-\mathbf{x}^{\boldsymbol{p}}(\boldsymbol{t})|}\times\boldsymbol{\alpha}^{p} \qquad (7)$$

$$\boldsymbol{u}_{\boldsymbol{\omega}}=\boldsymbol{\nabla}\,\mathrm{x}\,\Psi \qquad (8)$$

$$\nabla^{2}\Psi=-\boldsymbol{\omega} \qquad (9)$$

$$\boldsymbol{\nabla^{2}u}_{\boldsymbol{\omega}}=-\boldsymbol{\nabla}\times\boldsymbol{\omega} \qquad (10)$$

With the preliminary equations now summarized, the computation of the terms on the right hand side (RHS) of the evolution Equations 4 and 5 for the particle positions and strengths can be compared from the perspective of the Particle Strength Exchange (PSE) and Immersed Boundary Vortex-in-Cell (IB-VIC) methods.

2.1) Particle Strength Exchange (PSE) Method

In the Particle Strength Exchange (PSE) method, gradient operators are transformed into integral approximations using Green's function transformations [7], and this leads to additional particle-particle interactions with a naïve $O(N^2)$ scaling to compute the gradient terms. The PSE method permits particle strengths to be updated by stretching and diffusion within a single time step. The PSE method is mesh free by design; therefore, the particle-particle interactions (e.g. for the velocity field calculation) is typically obtained using treecodes or fast multipole methods which improve scaling to O(NlogN) and O(N) respectively. In this present study, the PSE results evaluated the velocity field using the direct $O(N^2)$ approach, Equation 7. The evolution of particle strengths, Equation 5, was then computed using the "transpose" PSE scheme with "high order algebraic smoothing kernel" as derived by Winckelmans & Leonard [7]. This computationally efficient PSE formulation [7] is attractive because it contains closed form diagnostics for kinetic energy, enstrophy, and helicity, which are useful diagnostics during code development and debugging. The PSE scheme is formulated as a mesh free method, but PSE also requires occasional remeshing of particles for stability. To maintain the self-adaptivity of the Lagrangian formulation without loss of accuracy due to particle distortions, particles are periodically remapped onto regular grid locations; i.e. "remeshed"—thus ensuring convergence of the method and enabling simulations to run for longer physical times without divergence. The remeshing step suppresses any spurious vortical structures that would otherwise appear in the

subgrid scale [8,9]. In the PSE and VIC methods, a background Cartesian mesh also provides a convenient means to facilitate particle remeshing, subgrid-scale models, and construction of flow visualizations.

2.2) Immersed Boundary Vortex-in-Cell (IB-VIC) Method

In the Vortex-in-Cell (VIC) method, terms involving differential operators (velocity gradient and vorticity diffusion) are computed efficiently on a Cartesian mesh using finite differences, and quantities defined on the mesh are transferred to the particles, and vice versa, using high-order moment conserving interpolation schemes. A uniform mesh also enables an efficient solution of the Poisson equation for the velocity field. The velocity field is obtained by solution of the Poisson Equation 10 using the approach of Hejlesen et al. [13] based upon FFTs and Green's function solution to Poisson's equation subject to free-space ($\boldsymbol{\omega}(\boldsymbol{r} \Rightarrow \infty) = 0$) or periodic boundary conditions. The use of Fast Fourier Transform (FFT) Poisson solver reduces the cost of obtaining the velocity field to O(NlogN). A viscous splitting algorithm (so-called fractional step) separates modification of particle strengths (Equation 5) into two sub-steps: an inviscid and then viscous time step—thus updating the particles through stretching and then diffusion sequentially. The motivation for using a viscous splitting algorithm is the possibility to satisfy wall-slip (inviscid) boundary conditions at solid surfaces through integral boundary element methods (IBEM) which supply the irrotational component $\boldsymbol{\nabla}\Phi$ of the Helmholtz decomposition [8]—although the IBEM is not yet included in this present study.

In this present study, the no-slip boundary condition at solid surfaces is imposed by adding the Brinkman penalization [12,14] term to the Navier-Stokes equations—referred to as the Immersed Boundary Vortex-in-Cell (IB-VIC) method. The idea of Brinkman penalization is that solid boundaries can be modeled 'in the limit' of zero porosity by penalizing the velocity field at the immersed fluid-solid interface. With Brinkman penalization [12,14], Equation 1 becomes

$$\frac{D\boldsymbol{\omega}}{Dt} = \boldsymbol{\omega} \cdot \boldsymbol{\nabla}\mathbf{u} + \nu\boldsymbol{\nabla}^2\boldsymbol{\omega} + \lambda\boldsymbol{\nabla} \times [\chi(\boldsymbol{u_s} - \boldsymbol{u})] \quad (11)$$

where χ is the solid mask identifying the separation of fluid and solid domains (0 in the fluid and 1 inside the solid), and $\boldsymbol{u_s}$ is the solid velocity. The solid mask is defined on a Cartesian mesh and constructed of a modified step function (a function of the signed distance to the solid surface) that varies smoothly (continuous and differentiable) in the direction normal to the surface [12]. The penalization parameter λ corresponds to an inverse porosity (units [s^{-1}]), and its value is restricted by a factor proportional to the inverse time step, $\lambda \leq\approx 1/\Delta t$ to ensure numerical stability. In the IB-VIC method, the gradients in the penalization term are also calculated using finite difference formulas on a uniform Cartesian mesh.

The VIC algorithm combined with Brinkman penalization technique offers an efficient way to capture effects of vortex shedding and fluid structure interaction. The immersed boundary approach greatly simplifies creation of meshes for immersed solids by decoupling the surface boundaries and computational mesh. However, a significant weakness of immersed boundary methods is that the near-surface boundary layer is highly unresolved due to the coarse uniform Cartesian mesh and choice of smoothing of the velocity field between the fluid-solid interface.

3. SAMPLE RESULTS

The numerical simulations presented in this work have been carried out using two vortex particle implementations. First, a Matlab code was developed to simulate the previously mentioned Particle Strength Exchange (PSE) method of Winckelmans & Leonard [7]. Although this PSE implementation used direct $O(N^2)$ approach for velocity evaluation, vectorization of code and GPU acceleration via Matlab Parallel Toolbox provided ~50x speedup compared to standard serial CPU implementation (observed for up to $O(10^4)$ particles). This PSE code was used to simulate the dynamics of vortex rings and wind/water turbines under dynamic inflow. Next, the method combining Vortex-in-Cell (VIC) algorithm with the Brinkman penalization approach of Rasmussen et al. [12] was used to simulate flow over bluff bodies and a 3D wing. This Fortran VIC code utilizes the Parallel Particle-Mesh (PPM) library [10], aiming towards massively parallel simulations.

3.1 PSE: Vortex Rings

Vortex rings are simple 3D vortex structures that provide interesting examples of non-linear interaction in flows with concentrated vorticity. Studying the dynamics of vortex rings serves as a useful benchmark during code development to verify accuracy and efficiency of the simulation code. Figure 2 illustrates the initialization of a two vortex rings on a uniform Cartesian grid, using a Gaussian shaped vorticity distribution over the core of the vortex rings. The "leapfrogging" vortex

ring phenomenon simulated by the PSE method is visualized in Figure 2 with a volume rendering of the vorticity field and particle trajectories. The rings are initialized with ~8,000 particles each and with circulation based Reynolds number $Re_\Gamma = \Gamma/\upsilon = 2000$. The simulation begins with two distinct vortex rings (Fig. 2 first row) and ends with breakup of the rings due to instabilities (Fig. 2 last row). The simulation captures fusion of the rings as the trailing vortex ring is pulled through the leading ring, followed by the development of azimuthal instabilities in the rings which leads to breakup and further dissipation of the rings. This particular simulation was performed without remeshing, and numerical blowup occurred shortly after the last frame shown in Figure 2. This is due to particle distortion, as referred in the previous section. Remeshing, vorticity redistribution and other techniques [7,9] can stabilize the method and allow longer simulation times with improved accuracy.

3.2 PSE: Turbines with Synthetic Turbulence

Vorticity generation and creation of wake flows within wind and tidal energy farms is a by-product of energy extraction. The PSE code described previously was setup to simulate vertical-axis and horizontal-axis tidal turbines in unsteady flow, as illustrated in Figure 4. The vorticity generated by turbine rotors is modeled using the lifting line and blade element approach, in which the vorticity produced by a turbine blade is lumped into a single line representing the lifting surface. A lifting line is subdivided into blade elements requiring look-up tables for the lift and drag coefficients of the rotor hydrofoils. After determination of the local induced velocity and flow angle, the bound circulation and lift force are related by the Kutta-Joukowski theorem. The bound circulation distribution along the lifting line is discretized using vortex particles, and as the rotor revolves, the particles are shed from the blade as a vortex sheet into the wake. The wake structure is fully discretized by vortex particles, which allows greatest flexibility for the wake structures to transition into the ambient flow. Blade element methods typically employ a number of ad-hoc corrections to account for additional rotational, unsteady, and other flow curvature phenomena—e.g. models for stall-delay, dynamic-stall hysteresis, cascade and tip/hub effects. In this preliminary work, the lifting-line method is simplified and such corrections are not yet implemented.

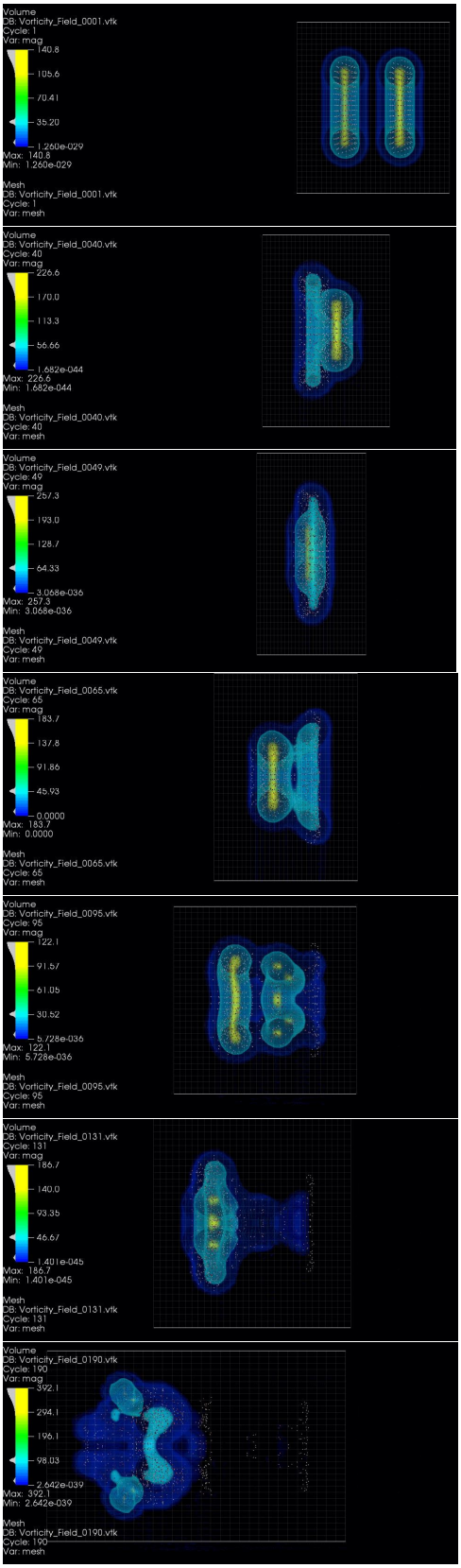

FIGURE 2. EVOLUTION OF LEAPFROGGING VORTEX RINGS. PARTICLES ARE COLORED BY CIRCULATION MAGNITUDE, OVERLAID WITH VOLUME RENDERING OF VORTICITY FIELD MAGNITUDE.

In the particular simulations of Figure 4, the bound circulation is simply prescribed along the blades to test the basic feature of adding rotating immersed lifting-lines to the PSE method. It provided a useful benchmark for testing how often remeshing should be performed; in this experiment the method is stable without remeshing for several rotations of the rotor until numerical blowup occurs. It is recommended that remeshing be performed as often as every time step, or as needed to control numerical error.

In order to simulate the effect of ambient turbulence, vorticity is introduced into the domain through the inlet plane by injecting vortex particles whose strengths induce a velocity field matching energy spectra characteristic of ambient-flow turbulence. The TurbSim method [4, 15] was used to pre-compute a spatial time-series (a sequence of 2D planes) that are statistically similar to real oceanic turbulence, shown in Figure 3. The turbulent inflow produces time-series with energy spectra, spatial coherence, mean profile, TKE profile, and Reynold's-stress profiles that are similar to real marine/river turbulence [15]. The pre-computed turbulent velocity field is convected through the inlet boundary with the mean flow speed, and then converted to vortex particles through a remeshing procedure (i.e. vorticity redistribution). The particles are then free to evolve according to the same PSE scheme as the vorticity modeled by the lifting line method.

Figure 4 shows the evolution of the wake over ~2 rotations of the rotors. These preliminary simulations contained ~50,000 particles by the end of simulation, and the basic structure of the helical wake and vortex roll-up in the hub and blade tip regions is present. Next, a turbulent velocity field was pre-computed using the TurbSim approach. Figure 3 illustrates the spatiotemporal flow that feeds into vortex method. Figure 4c illustrates how the turbulent inflow (from TurbSim) enters the vortex method domain as vortex particles. The inflow and wake particles evolve according to the same PSE algorithm, simulating the mixing of turbine wakes with ambient turbulence. Based on the input parameters of these PSE simulations, the Reynolds number based on the blade chord $Re_c = {U_\infty c}/{\upsilon}$ varies between 1-to-5 million, and the rotor diameter Reynolds number $Re_c = {U_\infty D}/{\upsilon}$ is approximately 20 million.

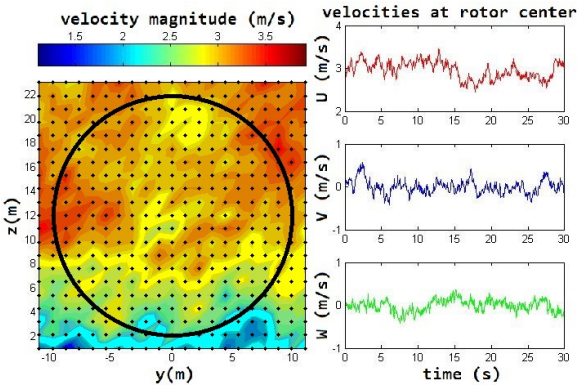

FIGURE 3. ILLUSTRATION OF THE VELOCITY FIELD FLUCUATIONS OVER SPACE (LEFT) AND TIME (RIGHT), REPRESENTING THE FLOW VARIATION OVER THE ROTOR DISK. THE TIME SERIES WAS GENERATED TO REPLICATE CONDITIONS IN PUGET SOUND, WASHINGTON, USA.

3.3 IB-VIC: 3D Wing

Finally, the Immersed Boundary Vortex-in-Cell (IB-VIC) method of Rassmussen et al. [12] combined with Brinkman penalization was implemented to simulate a 3D wing with NACA 4415 profile. The wing was simulated at zero incidence angle and chord based Reynolds $Re_c = 2000$ (Figures 5 and 6) and $Re_c = 10000$ (not shown). Simulations were performed using a 256 x 128 x 128 mesh, with dimensions [8c, 4c, 4c] so the VIC domain is spaced tightly around the vorticity support. Remeshing was performed at every cycle and the IB-VIC method remained stable over the duration of the simulations. For the $Re_c = 2000$ case, the time step was chosen as dt=0.1 seconds and the simulation of 20 seconds physical time took approximately 8 hours on a single CPU requiring ~30 GB of data total to save the velocity and vorticity fields at each cycle. In the $Re_c = 10000$ case, the time step was decreased to dt=0.05 seconds which doubled the computational time and storage required. Periodic boundary conditions were used to observe how vortex structures entering from the inlet will impact directly with the airfoil, causing further unsteady loading. However, the recycled inflow will contain time and length scales characteristic of the airfoil vortex shedding. It is desired for the inflow to have the characteristics of ambient turbulence; therefore, coupling the VIC method with synthetic turbulence generation is a direction of future interest [16].

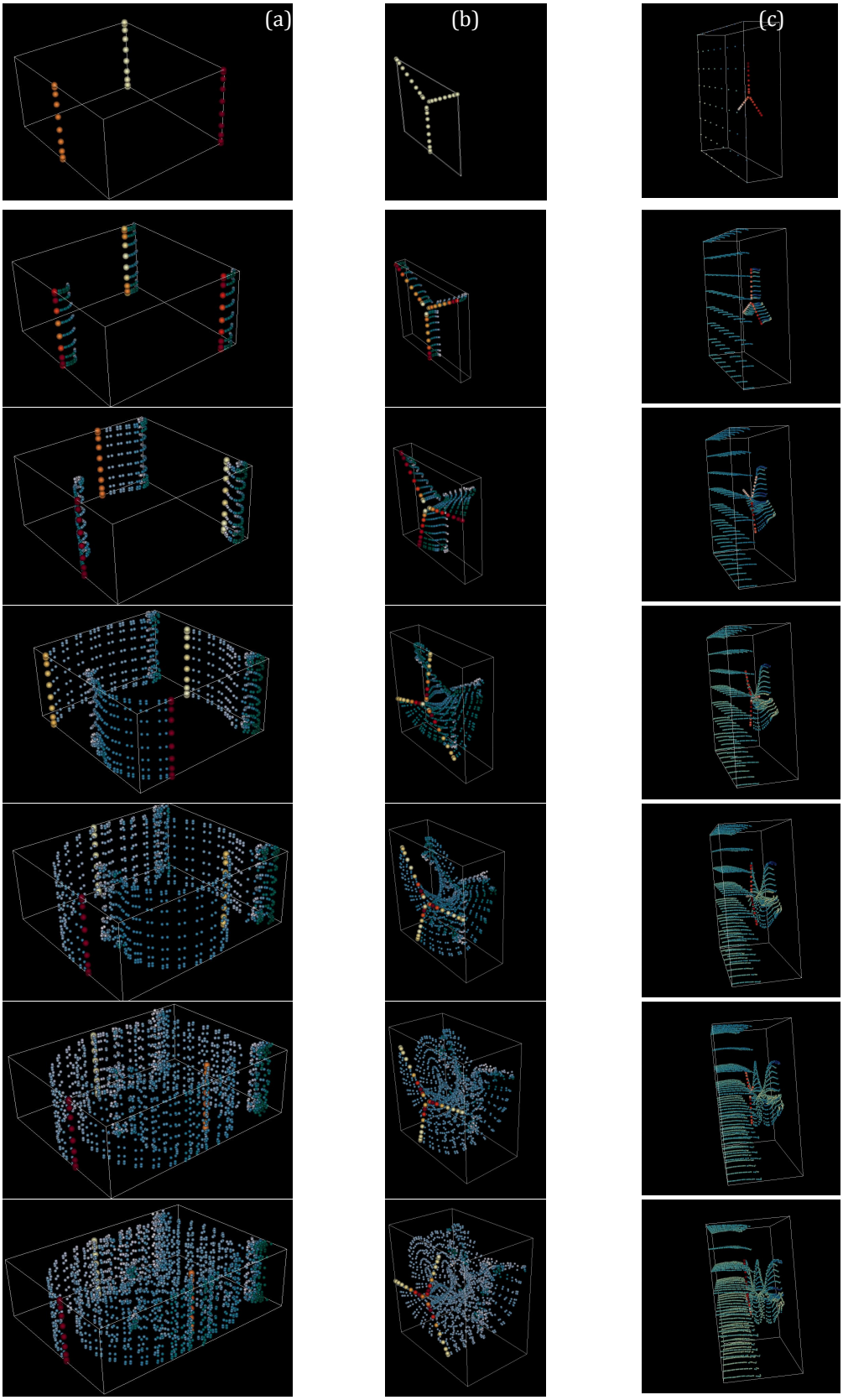

FIGURE 4. WAKE EVOLUTION OF VERTICAL-AXIS (A) AND HORIZONTAL-AXIS (B & C) HYDROKINETIC TURBINES BY PSE METHOD. THE VORTEX PARTICLES ARE COLORED BY THEIR VELOCITY; RED-TO-WHITE INDICATES THE INDUCED VELOCITY AT THE BLADES, AND BLUE-TO-WHITE INDICATES PARTICLE VELOCITY IN THE WAKE. THE DOMAIN DYNAMICALLY FOLLOWS THE VORTICITY SUPPORT. A TURBULENT INFLOW (C) IS INTRODUCED FROM THE INLET BOUNDARY. THE AMBIENT FLOW IS DIRECTED FROM LEFT TO RIGHT.

Figure 5 (top) shows the vorticity field, which shows approximately where the vortex particles are most concentrated. The resulting velocity field, Figure 5 (bottom), highlights the complicated flow field resulting from the highly three-dimensional flow structures (shown in Figure 6). The vorticity generation at the airfoil surface results in an observable von Kármán vortex street in the wake. As the Reynolds number increases, the relevant flow structures to resolve become even smaller and mixing in the wake is greatly enhanced.

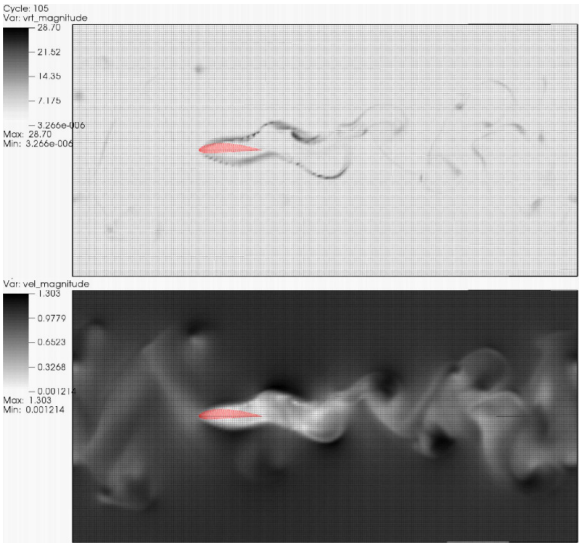

FIGURE 5. VORTICITY FIELD (TOP) AND VELOCITY FIELD (BOTTOM) FOR 3D FLOW OVER A NACA 4415 WING SHOWN AFTER IMPULSIVE START AND THE TRAILING EDGE VORTEX HAS RE-ENTERED THE DOMAIN DUE TO PERIODIC BOUNDARY CONDITION. $Re_c = 2000$

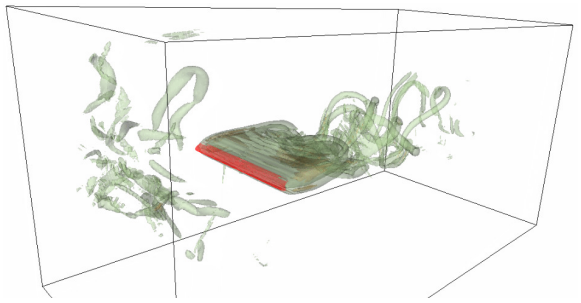

FIGURE 6. VORTICITY FIELD ISOSURFACES (GREEN) SHOWING VON KARMAN SHEDDING FROM THE AIRFOIL (RED) AND THEN REENTERING THE INLET FROM PERIODIC BOUNDARY CONDITIONS. $Re_c = 2000$

4. CONCLUSIONS

In this paper, the mathematical background and numerical procedure of the viscous vortex particle method is summarized, and the vortex particle methods are compared within the context of other CFD approaches. Some preliminary simulations are presented using the Particle Strength Exchange (PSE) and Immersed Boundary Vortex-in-Cell (IB-VIC) methods for vortex rings, wind / hydrokinetic turbines, and bluff body flows. To conclude, the initial experience of using this family of methods is summarized and the work ahead is outlined. The current simulations are a work in progress towards simulating the complex physics of tidal turbine flows; however, the effects of density stratification, tidal channel topography, tidal-cycle flow variation, or free-surface effects are not yet included. In geophysics flows, it can be inappropriate to apply the no-slip boundary condition to account for vorticity generation by terrain (i.e. the seabed); therefore a wall model could more efficiently handle viscous effects [5, 24]. Furthermore, for flat surfaces, the wall-slip Neumann boundary condition can be implemented easily using "image particles" in the vicinity of boundaries. Inclusion of the baroclinic vorticity generation could be implemented in which an additional set of particles carrying temperature are used to discretize an additional temperature equation based upon the Boussinesq approximation [9] (incompressible but with density variations proportional to temperature variations). The main challenge in the current work remains how to apply these vortex methods to higher Reynolds number flows for engineering applications such as wind and hydrokinetic turbines. To maintain a tractable amount of computational elements, sub-grid parameterization may be required to efficiently model the sub-particle scale dynamics. Adaptive mesh refinement is another worthwhile pursuit to achieve increased accuracy and reduce computational cost. Combining the immersed boundary and penalization techniques in the VIC algorithm allows fine vortex structures to be resolved near the solid boundaries; however, this comes with increased computational cost and an iterative correction method [20] is recommended for more accurate satisfaction of the no-slip boundary condition when the immersed boundaries are moving and accelerating. The immersed boundary method could be useful for modeling the vorticity from bluff bodies—such as the turbine nacelle or support structure. However, vorticity generation from the lifting surfaces (e.g. rotor blades) is modeled more efficiently using a lifting line / vortex lattice approach. Another promising option is to couple the vortex method to a more efficient near body solver, such as in [21] where a vortex method provides boundary conditions to a RANS solver with body-fitted mesh near the rotor blades.

To further assess the accuracy and efficiency of the developed vortex methods, future work will include comparisons to existing numerical and experimental studies of hydrokinetic turbines based on the DOE Reference Models [1, 22, 23].

Predictions of averaged flow fields, turbulence statistics, and unsteady loadings on turbine rotors and support structures will be essential to assess the usefulness of these particle methods. Essential directions for future work include the quantification of thrust, torque, power production, and wake characteristics.

ACKNOWLEDGEMENTS

The National Science Foundation (NSF) is thanked for providing the NSF Graduate Research fellowship to the first author under Grant No. DGE-0718124, and the Northwest National Renewable Energy Center is also thanked for supporting this work. Professors Brian Polagye, Jim Thomson, and James Riley provided many helpful discussions and guidance on this work. Johannes Tophøj Rasmussen and Mads Mølholm Hejlesen are greatly acknowledged for supplying code and guidance related to the FFT Poisson solver and PPM Library.

REFERENCES

[1] V. Neary, C. Hill, L. Chamorro, B. Gunawan, F. Sotiropoulos, "Experimental Test Plan – DOE Tidal and River Reference Turbines" Technical Report, Oak Ridge National Laboratory, 2012.

[2] Sanderse, B. and Pijl, S.P. and Koren, B.. "Review of computational fluid dynamics for wind turbine wake aerodynamics: Review of CFD for wind turbine wake aerodynamics" Wind Energy 2011, p. 799-819.

[3] Hansen, Martin OL and Aagaard Madsen, Helge. "Review paper on wind turbine aerodynamics" *J. Fluids Eng.* 133(11), 2011.

[4] Kelley, Neil Davis. "Turbulence-turbine interaction: the basis for the development of the TurbSim stochastic simulator" National Renewable Energy Laboratory, Technical Report, 2011.

[5] Churchfield, Matthew J. and Lee, Sang and Moriarty, Patrick J. and Martinez, Luis A. and Leonardi, Stefano and Vijayakumar, Ganesh and Brasseur, James G. "A large-eddy simulation of wind-plant aerodynamics." 50th AIAA Aerospace Sciences Meeting, Nashville, TN, 2012.

[6] Chatelain, Philippe, Backaert, Stéphane, Winckelmans, Grégoire & Kern, Stefan (2013). Large Eddy Simulation of Wind Turbine Wakes. *Flow Turbulence Combustion, 91*, 587-605.

[7] G. Winckelmans and A. Leonard, "Contributions to Vortex Particle Methods for the Computation of Three-dimensional Incompressible Unsteady Flows," *Journal of Computational Physics*, vol. 109, no. 2, pp. 247–273, Dec. 1993.

[8] G. Cottet and P. Koumoutsakos, Vortex methods: theory and practice, Cambridge University Press, 2000.

[9] G. Winckelmans. Vortex methods. Encyclopedia of Computational Mechanics, vol. 3. Wiley, New York (2004)

[10] I. F. Sbalzarini, J. H. Walther, M. Bergdorf, S. E. Hieber, E. M. Kotsalis, and P. Koumoutsakos. PPM – A Highly Efficient Parallel Particle-Mesh Library for the Simulation of Continuum Systems, *Journal of Computational Physics* 215(2):566-588, 2006.

[11] O. Awile, M. Mitrovic, S. Reboux, and I. F. Sbalzarini. A Domain-Specific Programming Language for Particle Simulations on Distributed-Memory Parallel Computers. In *Proc. III Intl. Conference on Particle-based Methods*, Stuttgart, Germany, September 2013.

[12] J. T. Rasmussen, G.-H. Cottet, and J. H. Walther, "A multiresolution remeshed Vortex-In-Cell algorithm using patches," *Journal of Computational Physics*, vol. 230, no. 17, pp. 6742–6755, Jul. 2011.

[13] M. M. Hejlesen, J. T. Rasmussen, P. Chatelain, and J. H. Walther, "A high order solver for the unbounded Poisson equation," *Journal of Computational Physics*, vol. 252, pp. 458–467, Nov. 2013.

[14] P. Angot, C.-H. Bruneau, P. Fabrie, A penalization method to take into account obstacles in incompressible viscous flows, Numer. Math. 81 (1999) 497–520.

[15] Thomson, J., L. Kilcher, M. Richmond, J. Talbert, A. deKlerk, B. Polagye, M. Guerra, and R. Cienfeugos (2013) Tidal Turbulence Spectra from a Compliant Mooring, *Proceedings of the 1st Marine Energy Technology Symposium*, April 10-11, 2013, Washington, DC.

[16] D. Kleinhans, R. Friedrich, A. P. Schaffarczyk, J. Peinke (2010) "Synthetic Turbulence Models for Wind Turbine Applications" Progress in Turbulence III Vol. 131, p. 111-114.

[17] J. Katz and A. Plotkin (2001) *Low-Speed Aerodynamics.* Cambridge University Press.

[18] P. Koumoutsakos (2005) "Multiscale Flow Simulations Using Particles" Annual Review of Fluid Mechanics Vol. 37: 457-487

[19] J. Murray and M. Barone (2011) The Development of CACTUS, a Wind and Marine Turbine Performance Simulation Code, AIAA, Orlando, FL.

[20] M. Hejlesen, P.Koumoutsakos, A. Leonard, and J. Walther (2013) An iterative penalization method for fluid/solid interfaces in vortex methods. Proc. of 26th Nordic Seminar on Comp. Mechanics

[21] C. Stone, E. Duque, C. Hennes, A. Gharakhani (2010) Rotor wake modeling with a coupled Eulerian and vortex particle method. AIAA, Orlando, FL.

[22] T. Javaherchi, N. Stelzenmuller, J. Seydel, A. Aliseda (2014) Experimental and Numerical Analysis of a Scale-Model Horizontal Axis Hydrokinetic Turbine, *Proc. of the 2nd Marine Energy Technology Symposium*, April 15-18, 2014, Seattle, WA.

[23] P. Bachant and M. Wosnik (2014) Reynolds Number Dependence of Cross-Flow Turbine Performance and Near-Wake Characteristics, *Proc. of the 2nd Marine Energy Technology Symposium*, April 15-18, 2014, Seattle, WA.

[24] M.J. Churchfield, Y. Li, P.J. Moriarty. A large-eddy simulation study of wake propagation and power production in an array of tidal-current turbines. *Phil. Trans. R. Soc. A 28 February 2013 vol. 371 no. 1985*